

Muscle redundancy is greatly reduced by the spatiotemporal nature of neuromuscular control

Brian A. Cohn^a and Francisco J. Valero-Cuevas^{a,b,2}

^aUniversity of Southern California, Department of Computer Science; ^bUniversity of Southern California, Department of Biomedical Engineering; Division of Biokinesiology and Physical Therapy

This manuscript was compiled on October 11, 2023

1 Animals must control numerous muscles to produce forces and movements with their limbs. Current theories of motor optimization and
2 synergistic control are predicated on the assumption that there are multiple highly diverse feasible activations for any motor task ('muscle
3 redundancy'). Here we demonstrate that the dimensionality of the neuromuscular control problem is greatly reduced when adding the temporal
4 constraints inherent to any sequence of motor commands: the physiological time-constants for muscle activation-contraction dynamics. We
5 used a 7-muscle model of a human finger to fully characterize the 7-dimensional polytope of all possible motor commands that can produce
6 fingertip force vector in any direction in 3D, in alignment with the core models of Feasibility Theory. For a given sequence of seven force
7 vectors lasting 300 ms, a novel single-step extended linear program finds the 49-dimensional polytope of all possible motor commands that can
8 produce the sequence of forces. We find that muscle redundancy is severely reduced when the temporal limits on muscle activation-contraction
9 dynamics are added. For example, allowing a generous 12% change in muscle activation within 50ms allows visiting only 7% of the feasible
10 activation space in the next time step. By considering that every motor command conditions future commands, we find that the motor-control
11 landscape is much more highly structured and spatially constrained than previously recognized. We discuss how this challenges traditional
12 computational and conceptual theories of motor control and neurorehabilitation for which muscle redundancy is a foundational assumption.

muscles | motor control | neuromuscular coordination

1 Controlling the muscles of a limb is a task 'cursed' by dimensionality, as it is a learning and control problem that requires
2 the nervous system to identify and implement a specific muscle coordination pattern from an infinite set of possible
3 options. Our objective in this work is to add more reality (constraints) to the models to uncover the way muscles 'must'
4 coordinate, given a task. This so-called *muscle redundancy* problem has been considered the central problem of motor control
5 in computational neuroscience for the past half-century (1).

6 There are three main conceptual approaches to this problem that attribute the nervous system the ability to mitigate
7 muscle redundancy by (i) *a priori* reducing the dimensionality of the problem to a handful of basis functions or 'synergies'
8 (e.g., (2–4)), (ii) defining cost functions to follow a gradient to find unique muscle coordination patterns (e.g., (5–7)), or (iii)
9 using experience-based sampling to find useful coordination patterns (e.g., Bayesian priors (8), trial-and-error (9), or habitual
10 (10)). Feasibility Theory (11, 12) contextualizes these alternative theories of neuromuscular control by formally describing the
11 high-dimensional set of all neuromechanically feasible coordination patterns. This is the landscape upon which all learning and
12 adaptation must take place at any point in time.

13 How a neural controller explores and exploits such high-dimensional landscapes is not known. But, from an anthropocentric
14 mathematical perspective (which may not be the way neural systems operate), it is computationally more tractable to use
15 optimization or dimensionality reduction than experience-based sampling, which may take an infeasibly long time in such

16 high-dimensional spaces (13, 14). Moreover, we and others have suggested that there may be non-obvious mechanical constraints
17 that must be considered when selecting coordination patterns such as the integrity of the joint (4, 15), or the instability of the
18 task (16, 17). In the case of rehabilitation, injury, and disease likely impose their own mechanical or dynamic constraints.

19 To find unique time-varying muscle coordination patterns in spite of the muscle redundancy problem, investigators use
20 dynamic optimization and optimal control formulations that enforce tenable (yet arbitrary) convex (generally quadratic) cost
21 function with differential equations that approximate the activation-contraction dynamics of muscle and equations of motion of
22 the limb (6, 7, 18–21). While this approach solves a well-posed mathematical problem, it does not, however, characterize the
23 redundancy problem the nervous system faces: **how** is the *dimensionality and structure* of muscle redundancy affected by the
24 neurophysiological time constants needed to change coordination patterns *over time*?

25 Synergy analyses are valuable for understanding the tendencies of muscles to collaborate and coordinate with one another,
26 across health and pathologies (22). In monitoring intermuscular coherence between muscles at the 10hz (alpha) range, specific
27 postures highlighted more alpha drive than others (23), suggesting that the task has a large effect on the way muscles coordinate
28 with themselves. In the effort to understand the ‘way’ muscles are coordinated, our drive is to clearly and exhaustively
29 characterize the task the neuromuscular system must be solving, so we can uncover the tenets of control. Muscle control and
30 body dynamics must be considered in parallel. This field of work aims to aid in our comprehension of the broader field of
31 comparative physiology and neuroscience, ultimately enhancing our knowledge of the biological underpinnings of movement in
32 diverse organisms and informing robotics, orthopedic, or prosthetic design for improved mobility and quality of life.

33 Here we describe how muscle activation-contraction dynamics, *a dynamical physiological constraint common to all time-*
34 *varying limb functions*, affects the dimensionality and structure of muscle redundancy. The dynamics of the limb and task
35 are as diverse as the multitude of behaviors, but the fact that muscles cannot change force level instantaneously affects the
36 options in the next moment (24, 25). We refer to this behavior as a ‘spatiotemporal tunnel’—the well-structured representation
37 of feasible muscle activations to achieve a series of isometric forces, where the limb must meet the force output across each
38 discretized moment in time (Fig 1). We provide a novel conceptual and computational approach to determine how muscle
39 activation-contraction dynamics limit the feasible changes in muscle activation pattern at a given point during a time-varying
40 force modulation task.

41 We demonstrate, using the sample task of redirecting a 10N fingertip force over a 30° arc (Fig 1), that we can characterize a
42 well-structured and lower-dimensional ‘spatiotemporal tunnel’ that contains the set of all feasible muscle activations without
43 invoking cost functions or performing *a priori* dimensionality reduction.

44 Results

45 We find that the time history of feasible activations for a time-varying task is highly restricted by the activation-contraction
46 dynamics imposed by muscle physiology (Fig 2).

47 As the activation-contraction speed limit is reduced, the trajectories become more spatially constrained in the regions of the
48 feasible activation space they can inhabit/exploit (Fig 2d). This allows us to describe the effects of the *activation-contraction*

Theory and computation by BAC. Experimental development and interpretation by BAC, FVC. Manuscript written by BAC, FVC.

No competing interests to report.

²To whom correspondence should be addressed. E-mail: valero@usc.edu

49 *constraint* under which muscle coordination happens to be able to produce a force and change its direction on the activation
50 levels across the task, activation-contraction speeds (Fig 2b), signed maximum activation-contraction speeds observed across
51 the larger pool of generated trajectories ($n=10,000$, Fig 2c), and the max-absolute-value activation-contraction speeds for
52 each muscle, across each activation-contraction constraint (Fig 2d). Some muscle trajectories appear more profoundly affected
53 by more stringent activation-contraction constraints than others, such as EIP, EDC, and LUM (Fig 2d). As the maximal
54 activation-contraction speed is reduced, those same muscles will visit/exploit increasingly smaller subspaces of their feasible
55 activation space. This spatiotemporal interaction is best seen in *EIP*, which has a naturally large range of feasible activation,
56 which are suitably exploited when the activation-contraction constraint is less-constraining. But then shrinks as the constraint
57 becomes more strict. However, changes also spill over to muscles with naturally smaller ranges of feasible activations such
58 as *FDP*. This muscle has few trajectories with an activation-contraction rate greater than 0.25 to begin with, but becomes
59 limited in range as the activation-contraction speed is reduced (Fig 2d).

60 A closer look further confirms that muscles that have a narrow range of feasible activations will be least sensitive to changes
61 in activation-contraction constraints. *FDP*, *FDS*, and *PI* are more affected by the reduction of maximal activation-contraction
62 speed—muscles which don't have much room to move are constrained primarily by their involvement in the task, and secondarily
63 by the activation-contraction constraints; the muscles that have greater ranges of activation have non-overlapping central
64 quartiles between the 0.75 and 0.5 activation-contraction constraint (Fig 2d).

65 Producing a fingertip force and changing its direction requires selecting a specific solution and implementing a specific
66 sequence of activation patterns. Our ‘seeded analysis’ reflects the consequences of choosing an initial activation pattern (a
67 ‘seed’) to subsequent feasible activation patterns. We examine the case where the first activation is fixed to a single option
68 (the unclamped case in Fig 3a) and the ‘clamped’ case, where the first and last activation must match one another (Fig 3b).
69 Given a seed, subsequent feasible activations for each muscle are highly limited in where they can go when unclamped, and
70 when clamped the activation trajectories have (by design) a symmetric expansion and contraction of the activation space.
71 Traditional techniques for visualizing these spaces, including density distributions and parallel coordinates as used in (11) could
72 be misleading on the raw activations when incorporating the concept of time.

73 Finally, the hypothesis illustrated conceptually in Figure 1 is highly supported by data in Figure 3. We show how, for
74 ten randomly selected seed points, the activation-contraction constraints shown in Figure 2a-b limit the evolution of muscle
75 activations over time in the force redirection task, and how the blue seeded point has its space limited to 7%. The 7% result is
76 when muscle activations are constrained to remain within 12% of its activation between each time slice (the highest allowable
77 activation change is set to 0.12 per 50ms).

78 To create an adequate visualization, we had to find a method to fairly represent, project, and render the 49-dimensional
79 space of trajectories onto a page as a 2D representation.

80 Given a starting point in $t = 0$, the time-constrained activations form a ‘tunnel’. A single seed point defines where the
81 activation must move, highly limiting the space of feasible activation patterns that can be used to achieve the rest of the task;
82 a spatiotemporal tunnel exists. Furthermore, when constraining the muscle activation trajectory to have identical starting and
83 finishing activation patterns as in Figure 3b, the muscle redundancy shrinks dramatically.

84 **Discussion**

85 The temporal constraints imposed by muscle activation-contraction dynamics greatly affect the neuromuscular control landscape
86 upon which all learning, motor control, and evolution must operate. This underappreciated aspect of muscle mechanics has
87 strong implications when navigating the feasible solution space for a task where a null space for control exists. In addition, this
88 approach challenges traditional computational and conceptual theories of motor control and neurorehabilitation for which
89 muscle redundancy is a foundational assumption.

90 Importantly, the range of valid solutions, i.e., muscle redundancy, does not necessarily decrease in light of activation-
91 contraction constraints, as the feasible activation space is defined by the anatomy of the limb and the operating constraints
92 of the task (12). In addition, the *utility* of a muscle has been described many times as a description of the bounds within
93 which that muscle can be used and can contribute (11, 26–28). Nevertheless, our work highlights how those bounds on
94 muscle redundancy are too optimistic for time-varying evaluations of spatiotemporal feasibility, even in a very simplistic force
95 redirection task. That is, just because a solution in the feasible activation space is valid, it does not mean that it is reachable
96 at any point in time. Rather, the possibility of implementing a new muscle coordination pattern in finite time is conditioned on
97 the current muscle coordination pattern.

98 As discussed in detail in (11, 12, 29), the concept of muscle redundancy has been interpreted to mean that the nervous
99 system is confronted with the computational need to solve an underdetermined problem that has infinite solutions. There are,
100 however, constraints other than those explicitly imposed by the force or movement production task that conspire to reduce the
101 dimensionality of the feasible activation space. For example, muscle coordination must consider anatomical constraints to
102 stabilize joints (4, 30) or regulate limb impedance (31)—which additionally reduce the feasible activation set. We now add the
103 critical aspect of *temporal constraints* imposed by muscle activation-contraction dynamics, further showing that the ‘problem’
104 of motor control is not as underdetermined as commonly proposed. Importantly, ‘reducing the dimensionality’ of the feasible
105 activation is synonymous with meeting an additional constraint (12). This additional spatiotemporal structure in time-varying
106 muscle activation patterns then further complicates the disambiguation of so-called *descriptive synergies* that arise naturally
107 from the structure imposed by the constraints of the task, from *prescriptive* ones that are proposed to be explicitly regulated
108 by the nervous system (12, 32–34).

109 Moving beyond the traditional view of muscle redundancy opens up exciting alternative perspectives to understand function,
110 disability, and rehabilitation. It is no longer necessary to continue to assume that optimization or dimensionality reduction
111 of motor signals is the only or primary *modus operandi* of the nervous system (11, 29, 35). For one, our work highlights the
112 important role the properties of muscle play in the co-evolution and co-adaptation of brain and body (36).

113 More broadly, our results point to the long-underappreciated hierarchical distributed architecture of the nervous system
114 (37–39): the time-history of muscle activations arises from the collaboration of slower cortical ‘higher-level’ circuits with faster
115 brainstem and spinal ‘lower-level’ circuits to manage perturbations and other time-critical interactions with the ground and
116 body mechanics. Thus, for example, stroke rehabilitation need not only focus only on disruptions of the corticospinal tracts
117 as they coordinate ‘redundant musculature.’ Rather, we can focus on potentially more clinically impactful approaches for
118 understanding the interactions across the neuroaxis to mitigate the known dysregulation of brainstem and spinal circuitry in
119 stroke (40–42) and the accompanying reduction in rate of force production (43) responsible for deficits in the time-sensitive

120 coordination of muscles.

121 At a practical clinical level, these findings improve our understanding of the impact of changes in the rate of muscle force
122 production on neuromuscular control, its deficits in clinical conditions, and their rehabilitation. The rate of muscle force
123 production is determined by the recruitment and rate coding of the motoneuron pool combined with activation-contraction
124 dynamics. The net rate of force production can, for a variate of reasons, be enhanced with training (44) or reduced by pain
125 (45), joint injury (46), Parkinson's disease (47), and stroke (43)—among other conditions. An impact on the feasible activation
126 space can be readily modeled by reducing the strength or speed of a given muscle with the same approach described herein.
127 Therefore, our results directly suggest that the ability to navigate the feasible activation space can be positively or negatively
128 affected by those muscle-level changes from training and clinical conditions, respectively.

129 This expanded perspective aligns more closely with the complexities of the co-evolution of neural, muscular, and anatomical
130 structures for effective control of real-world motor tasks with realistic muscle activation-contraction properties. In addition, it
131 offers a more comprehensive understanding of how the nervous system collaborates with muscle activation-contraction properties
132 to efficiently control function. Navigating these spatiotemporal landscapes, and how those landscapes change, is the physics
133 upon which animal brains and bodies co-evolved. Our work is thus conducive to cross-species comparisons of ‘spatiotemporal
134 tunneling’ in the context of evolutionary biology like, for example, when comparing the index finger manipulability between
135 humans and bonobos(48). Several cadaveric, computational, and *in vivo* studies then allow a wide variety of future comparisons
136 to support ongoing research into the control of numerous muscles (49, 50), and how it is further constrained by mechanics and
137 time (17).

138 Prior work in (11) directly shows the impact of reducing the strength of one muscle, and can show the relative loss of
139 volume for the resulting feasible activation space—the same analysis could be readily used with the spaces with additional
140 spatiotemporal constraints. For instance, consider a scenario where the strength of a few muscles is reduced by 50%, possibly
141 due to an acute injury. By utilizing models developed in this research, we can visually depict how the remaining muscles
142 might need to adjust to accommodate this altered motor capability while still achieving the same task performance. This can
143 offer valuable insights to clinicians and researchers, helping them better comprehend why even a minor injury can result in a
144 significantly different movement pattern. While the change in one muscle may seem small, it can render certain areas within
145 the range of feasible muscle activations inaccessible. Consequently, the patient will need to find a new solution or opt for a
146 different output force, such as adopting a new walking style.

147 We use an index fingertip as our ‘model organism’, and while fewer muscles are involved than for other limbs, there is a
148 path and some precedent for applying these techniques to higher-dimensional models, e.g. the entire posterior chain of a cat
149 (26). Adding activation-contraction dynamics into higher-dimensional systems can help us understand which constraints are
150 most influential in limiting the feasible activation space, and help us find which tasks may be more affected.

151 An important limitation of our work is that additional research is necessary fully apply our approaches to various scenarios
152 involving pseudo-static, slow, fast, and ballistic movements. We anticipate, however, that incorporating dynamic constraints
153 into our analysis will narrow down the range of feasible muscle activations and provide deeper insights into the actual limitations
154 governing the development and adaptation of motor control.

155 Ultimately, this paper calls for a measured re-evaluation of existing optimization- and synergy-based motor control theories to
156 better account for how the integrative neuroaxis operates as a hierarchical and distributed system to control the spatiotemporal

157 dynamics of muscle coordination. Producing a more accurate view of the physical system of constraints can aid in our
158 understanding of how motor control has evolved in animals.

159 **Materials and Methods**

160 As in (11, 26, 27) we define the linear transduction of tendon tensions into output endpoint wrench as

161
$$H * \bar{x} = \bar{w}. \quad [1]$$

162 Where H (a $[4, 7]$ matrix in this paper for 4 output dimensions and 7 input tendon activations) represents the linear activation-to-wrench
163 relationship, such that $H * x = \bar{w}_{output}$. We refer to wrench in the mechanical sense, where it represents the output forces and torques
164 produced at the endpoint—in this case, at the fingertip.

165 Wrenches are four-dimensional as the index finger can produce a torque (i.e. scratching) $\bar{w} = (f_x, f_y, f_z, t_y)$ (15). We show the output
166 forces, frame-of-reference, and the actual joint torques in Figure 1. As the data for H were collected in the same posture, and as there is
167 strong evidence supporting the linearity of tendon-driven isometric force transduction in fixed postures, we do not need to model the
168 intermediary Jacobian or the Moment-arm matrix (26, 30, 51, 52). We define $x \in [0, 1]^7$ where 1 represents 100% activation.

169 Note that the term ‘*muscle activation*’ can take on different meanings depending on the level of the analysis being used. In our case,
170 we use it as shorthand for the total signal needed to produce a given level of neural drive to produce force at each muscle. The reason we
171 do this is that it encompasses the metabolic cost, intensity, and feasible rates of change of both the neural drive and muscle force. As such,
172 it includes:

- 173 • Presynaptic input to a population of α -motoneurones
- 174 • The neural command sent by the α -motoneuron to the population of muscle fibers in its motor units (53)
- 175 • The biochemical processes required for the release and uptake of acetylcholine at the motor end-plate of each muscle fiber (54)
- 176 • Ca^{2+} release and uptake by the *sarcoplasmic reticulum* (54)
- 177 • The cross-bridge cycle at the sarcomere to produce, hold and change the level of muscle force

178 We make the simplification, without loss of generality, to not distinguish between muscle types and consider equal time constants for
179 the increase and decrease of neural drive and muscle force. And while many approaches minimize $\bar{c}^T \bar{x}$ where \bar{c} represents a vector of
180 linear weights to combine with \bar{x} to form a metric of cost, e.g. if $\bar{c} = (1, 1, 1, 1, 1, 1, 1)$, $\bar{c}^T \bar{x}$ would compute the ‘sum cost of activation’, or
181 $\bar{c} = (0, 0, 0, 0, 0, 0, 1)$ would compute the ‘sum of just *palmar interosseus*’. Nonlinear objective functions have also been used to better
182 understand weighted L_2 and L_3 metabolic cost functions(11). For this paper, rather than minimization or optimization on an arbitrarily
183 defined cost function (a model choice in itself) our approach instead **samples from the nullspace** of \bar{x} uniformly-at-random (*u.a.r*). We
184 leverage the same computational geometry technique ‘Hit-And-Run’ as in (11, 27), which is originally described in (13).

185 Synaptic drive applied to motor units create forces, which ultimately generate muscle forces, and accumulate to tendon force. The
186 tendon is compliant and together, the musculotendon is a big dynamic system with many physiological and physical constraints. It’s a
187 series elastic element.

188 **Hit and Run sampling of the feasible activation space.** Visualization and analyses of these high dimensional structures requires unique
189 approaches to highlight different aspects of feasible activation spaces, and there has been some success in using 2D and 3D visualization
190 to decompose neural control of force (11, 27). As the dimensionality of the space increases, the ratio of out-of-polytope to in-polytope
191 volumes within the unit cube expands exponentially, thereby making 2D and 3D approaches computationally intractable with systems
192 with more than 2 muscles. Like in prior work, we sample the space with the Hit-and-Run algorithm—a Markov chain propagating within
193 the polyhedron that yields a uniform-at-random distribution within the volume of a given convex polytope. This method is agnostic to
194 measures of metabolic or neurologic cost, and allows for contextualization of the solutions optimization may select.

195 **Defining the temporal constraints.** One core limitation of our prior work (11) is the single-moment analysis, that does not take into account
 196 the amount of change the CNS must perform to move from solution to solution, from task to task. Muscles do not act with infinitely fast
 197 response times; to respect this, we incorporate an element of temporal constraint in our model by limiting a muscle's change in activation
 198 between $\pm\delta\%$ over a 50ms interval. Given the observation that deactivation in vertebrate muscle is often slower than activation(53), we
 199 set this limit to the faster of the two, forming a conservative bound. We refer to this metric as the activation-contraction constraint,
 200 and as we take the absolute value of the deltas, this metric is always set between [0, 1]. A constraint value of 0.25 means that in 50ms,
 201 activations can change their output by no more than 25% of their maximal tension.

202 **Specimen.** Our activation-to-wrench model H was sourced from an experiment using cadaver fingers(55), with original data ($n=11$) from
 203 (56). To reveal the effects of activation-contraction constraints on a time-dependent feasible activation space, we leveraged a stochastic
 204 Monte Carlo technique to fairly extract activation trajectories—Hit-and-Run(13). In addition to being normalized between an activation
 205 of 0 and 1 (muscles can't go negative as they can only pull), muscles were constrained in their ability to change their output activation
 206 from moment to moment. For each moment in time, the endpoint vector had to meet the requirements of its desired output wrench
 207 within a series of seven tasks. Formally, we add new constraints in the way the activations can change, which are ultimately classifiable as
 208 Lipschitz constraints (57, 58). Formally, we sample $u.a.r.$ (uniformly at random) from the null space on x , given A and b where $x \in [0, 1]^n$.
 209 Our Lipschitz Constraints (referred to hereafter as ‘activation-contraction constraints’ as they serve to link different motor patterns over
 210 time to different output wrenches.

$$211 \quad |x_{i+1} - x_i| \leq \delta x \in [0, 1]^7 \quad [2]$$

$$212 \quad \begin{pmatrix} f_x \\ f_y \\ f_z \\ \tau_y \end{pmatrix} = \mathbf{w} = H\mathbf{a} = H \begin{pmatrix} a_1 \\ a_2 \\ a_3 \\ \dots \\ a_7 \end{pmatrix}, \mathbf{a} \in [0, 1]^7 \quad [3]$$

213 We set the task to a series of 7 individual wrenches performed over the course of 300ms, which starts at a pure f_x force (towards palmar),
 214 with a 30 degree rotation towards proximally (rotated about the axis defined by the ulnar direction), and a symmetrical return. The
 215 progress is shaped as a single cosine period, with the peak being the 4th index. Wrenches ($w_{t=0} = w_{t=6}$),($w_{t=1} = w_{t=5}$),($w_{t=2} = w_{t=4}$)
 216 are identical—providing a symmetric set of tasks to stay constant while the activation-contraction constraint demands may change.

217 **Method for generating unseeded and seeded trajectories** Unseeded trajectories can originate in any valid solution at $t = 0$
 218 show their evolution across the subsequent polytopes (i.e., solution spaces) subject to the temporal constraints of activation-contraction
 219 dynamics of muscle. A seeded trajectory, on the other hand, is pulled from the same constraint matrix, but with an additional constraint:
 220 all of the points selected from a seed start at a same seed point (i.e., valid solution at $t = 0$). A seed point can be extracted from the
 221 unseeded trajectories. Seeded points can only evolve in time into subregions of the subsequent solution spaces that are reachable given the
 222 starting point *and* the temporal constraints of activation-contraction dynamics of muscle. Importantly, unseeded trajectories all meet
 223 activation-contraction constraints as well.

224 **Quantifying the evolution over time of the distribution of solutions for unseeded and seeded trajectories.** Here we detail our method for
 225 analyzing and visualizing the effect of selecting a solution seeded in $t = 0$. We began by extracting one hundred thousand activation
 226 trajectories from H (Eq. 3). With 10 of those trajectories, we extracted only the first value, then ran a further sampling paradigm on a
 227 modified constraint equation where the first activation pattern (of 7 muscle activations) had to match the seed's activations at $t = 0$
 228 (unclamped) and another case where the $t = 0$ and $t = 300$ had to match (clamped). As we want to visualize the effect of selecting a
 229 seed point, but cannot easily plot a 4D structure embedded in 7D, we applied principal component analysis to each of the 7 moments of
 230 time across the unseeded distribution. We then projected both the unseeded, and seeded activation trajectories across the first two PCs,
 231 highlighting where in the lower-dimensional space those solutions were most probable.

232 We sampled 100,000 activation trajectories per activation-contraction constraint condition, where the constraints were set from 1 to

233 0.05.

234 **Seeded and Unseeded analyses.** To address this difficulty in analyzing the distributions of muscle activations, we present the following
235 ‘unseeded vs seeded’ trajectory analysis in Figure 3. We compute the possible trajectories when the first moment is fixed to a seed-point,
236 and compare those ‘seeded’ trajectories to the ‘unseeded’ trajectories that were not fixed. Unseeded trajectories are still sampled under
237 the same activation-contraction constraint as their seeded counterpart, that all unseeded trajectories meet the activation-contraction
238 constraint, and that all seeds must have a starting point that exists in the unseeded polytope. For the ‘clamped’ case, we require the
239 starting and ending point activations to match one another. To pick good seed points that would generate viable trajectories, we computed
240 100,000, filtered by those that met an activation-contraction constraint of 0.12, and selected 10 at random as our ‘seeds’. For each seed,
241 we trimmed off the $t = 50$ to $t = 300$ activation values, and appended a new constraint to the original constraint matrix, so all sampled
242 trajectories had an additional constraint to match the seed in $t = 0$. Finally, to evaluate the effect of adding this constraint, we examine
243 the $t = 50$ time step between the seeded and unseeded case, tracing the 2D convex hull of the PNG image in pixels (ImageJ (59)). The
244 inner area (seeded case) of $8972px^2$ divided by the outer area (unseeded case) $126926px^2 = 7\%$.

245 **ACKNOWLEDGMENTS.** We thank C Laine and H Narayanan for their support in the refinement of the neurophysiological implications
246 and theoretic implementations of this work.

- 247 1. Bernstein N. The co-ordination and regulation of movements. The co-ordination and regulation of movements. 1966:.
- 248 2. Alessandro C, Delis I, Nori F, Panzeri S, Berret B. Muscle synergies in neuroscience and robotics: from input-space to task-space perspectives. Frontiers in computational neuroscience. 2013;7.
- 249 3. Tresch MC, Jarc A. The case for and against muscle synergies. Current opinion in neurobiology. 2009;19(6):601–607.
- 250 4. Alessandro C, Barroso FO, Prashara A, Tentler DP, Yeh HY, Tresch MC. Coordination amongst quadriceps muscles suggests neural regulation of internal joint stresses, not simplification of task
251 performance. Proceedings of the National Academy of Sciences. 2020;117(14):8135–8142.
- 252 5. Chao EY, An KN. Graphical Interpretation of the Solution to the Redundant Problem in Biomechanics. Journal of Biomechanical Engineering. 1978;100(3):159–167. doi:10.1115/1.3426207.
- 253 6. Anderson FC, Pandy MG. A dynamic optimization solution for vertical jumping in three dimensions. Computer methods in biomechanics and biomedical engineering. 1999;2(3):201–231.
- 254 7. Todorov E, Jordan MI. Optimal feedback control as a theory of motor coordination. Nature neuroscience. 2002;5(11):1226–1235.
- 255 8. Kording KP, Wolpert DM. Bayesian integration in sensorimotor learning. Nature. 2004;427(6971):244–247.
- 256 9. Adolph KE, Cole WG, Komati M, Garciaguire JS, Badaly D, Lingeman JM, et al. How do you learn to walk? Thousands of steps and dozens of falls per day. Psychological science. 2012;23(11):1387–
257 1394.
- 258 10. De Rugy A, Loeb GE, Carroll TJ. Muscle coordination is habitual rather than optimal. The Journal of Neuroscience. 2012;32(21):7384–7391.
- 259 11. Cohn BA, Szedlák M, Gártner B, Valero-Cuevas FJ. Feasibility theory reconciles and informs alternative approaches to neuromuscular control. Frontiers in computational neuroscience. 2018;12:62.
- 260 12. Valero-Cuevas FJ. Fundamentals of Neuromechanics. vol. 8 of Biosystems and Biorobotics. SpringerVerlag London; 2016.
- 261 13. Lovász L. Hit-and-run mixes fast. Mathematical Programming. 1999;86(3):443–461.
- 262 14. Chen Y, Dwivedi R, Wainwright MJ, Yu B. Fast MCMC sampling algorithms on polytopes. The Journal of Machine Learning Research. 2018;19(1):2146–2231.
- 263 15. Valero-Cuevas FJ, Zajac FE, Burgar CG. Large index-fingertip forces are produced by subject-independent patterns of muscle excitation. Journal of biomechanics. 1998;31(8):693–703.
- 264 16. Johanson ME, Valero-Cuevas FJ, Hentz VR. Activation patterns of the thumb muscles during stable and unstable pinch tasks. J Hand Surg Am. 2001;26:698–705.
- 265 17. Sharma N, Venkadesan M. Finger stability in precision grips. Proceedings of the National Academy of Sciences. 2022;119(12):e2122903119.
- 266 18. Falisse A, Serrancoli G, Dembia CL, Gillis J, De Groote F. Algorithmic differentiation improves the computational efficiency of OpenSim-based trajectory optimization of human movement. PloS one.
267 2019;14(10):e0217730.
- 268 19. Rahmati M, Rostami M, Beigzadeh B. A low-cost optimization framework to solve muscle redundancy problem. Nonlinear Dynamics. 2017;90(4):2277–2291.
- 269 20. Sohn MH, Smith DM, Ting LH. Effects of kinematic complexity and number of muscles on musculoskeletal model robustness to muscle dysfunction. PLOS ONE. 2019;14(7):e0219779.
270 doi:10.1371/journal.pone.0219779.
- 271 21. Simpson CS, Sohn MH, Allen JL, Ting LH. Feasible muscle activation ranges based on inverse dynamics analyses of human walking. Journal of Biomechanics. 2015;48(12):2990–2997.
272 doi:10.1016/j.jbiomech.2015.07.037.
- 273 22. Turpin NA, Uriac S, Dalleau G. How to improve the muscle synergy analysis methodology? European journal of applied physiology. 2021;121(4):1009–1025.
- 274 23. Laine CM, Cohn BA, Valero-Cuevas FJ. Temporal control of muscle synergies is linked with alpha-band neural drive. The Journal of physiology. 2021;599(13):3385–3402.
- 275 24. Venkadesan M, Valero-Cuevas FJ. Neural control of motion-to-force transitions with the fingertip. Journal of Neuroscience. 2008;28(6):1366–1373.
- 276 25. Keenan KG, Santos VJ, Venkadesan M, Valero-Cuevas FJ. Maximal voluntary fingertip force production is not limited by movement speed in combined motion and force tasks. Journal of Neuroscience.
277 2009;29(27):8784–8789.

- 278 26. Sohn MH, McKay JL, Ting LH. Defining feasible bounds on muscle activation in a redundant biomechanical task: practical implications of redundancy. *Journal of Biomechanics*. 2013;46(7):1363–1368.
- 279 doi:10.1016/j.jbiomech.2013.01.020.
- 280 27. Valero-Cuevas F, Cohn B, Szedlák M, Fukuda K, Gärtner B. Structure of the set of feasible neural commands for complex motor tasks. In: Conference proceedings of the Annual International Conference of the IEEE Engineering in Medicine and Biology Society. IEEE Engineering in Medicine and Biology Society. Annual Conference. vol. 2015. NIH Public Access; 2015. p. 1440.
- 282 28. J VCF, A CB, F YH, L LE. Exploring the high-dimensional structure of muscle redundancy via subject-specific and generic musculoskeletal models. *J Biomech*. 2015;In press.
- 283 29. Mulla DM, Keir PJ. Neuromuscular control: from a biomechanist's perspective. *Frontiers in Sports and Active Living*. 2023;5.
- 284 30. Valero-Cuevas FJ, Zajac FE, Burgar CG. Large index-fingertip forces are produced by subject-independent patterns of muscle excitation. *J Biomed*. 1998;31:693–703.
- 285 31. Inouye JM, Valero-Cuevas FJ. Muscle synergies heavily influence the neural control of arm endpoint stiffness and energy consumption. *PLoS Comput Biol*. 2016;12(2):e1004737.
- 286 32. Brock O, Valero-Cuevas F. Transferring synergies from neuroscience to robotics: Comment on "Hand synergies: Integration of robotics and neuroscience for understanding the control of biological and artificial hands" by M. Santello et al. *Physics of life reviews*. 2016;17:27–32.
- 288 33. Bruton M, O'Dwyer N. Synergies in coordination: A comprehensive overview of neural, computational, and behavioral approaches. *Journal of neurophysiology*. 2018;120(6):2761–2774.
- 289 34. Kutch JJ, Valero-Cuevas FJ. Challenges and new approaches to proving the existence of muscle synergies of neural origin. *PLoS computational biology*. 2012;8(5).
- 290 35. Loeb GE. Optimal isn't good enough. *Biological cybernetics*. 2012;106(11-12):757–765.
- 291 36. Valero-Cuevas FJ, Erwin A. Bio-robots step towards brain–body co-adaptation. *Nature Machine Intelligence*. 2022;4(9):737–738.
- 292 37. Loeb GE, Brown IE, Cheng EJ. A hierarchical foundation for models of sensorimotor control. *Exp Brain Res*. 1999;126(1):1–18.
- 293 38. Windhorst U. Muscle proprioceptive feedback and spinal networks. *Brain research bulletin*. 2007;73(4-6):155–202.
- 294 39. Kudithipudi D, Aguilar-Simon M, Babb J, Bazhenov M, Blackiston D, Bongard J, et al. Biological underpinnings for lifelong learning machines. *Nature Machine Intelligence*. 2022;4(3):196–210.
- 295 40. Finley JM, Perreault EJ, Dhaher YY. Stretch reflex coupling between the hip and knee: implications for impaired gait following stroke. *Experimental brain research*. 2008;188:529–540.
- 296 41. Lan Y, Yao J, Dewald JP. The impact of shoulder abduction loading on volitional hand opening and grasping in chronic hemiparetic stroke. *Neurorehabilitation and neural repair*. 2017;31(6):521–529.
- 297 42. Li S, Francisco GE. New insights into the pathophysiology of post-stroke spasticity. *Frontiers in human neuroscience*. 2015;9:192.
- 298 43. Naik SK, Patten C, Lodha N, Coombes SA, Cauraugh JH. Force control deficits in chronic stroke: grip formation and release phases. *Experimental brain research*. 2011;211:1–15.
- 299 44. Blazevich AJ, Wilson CJ, Alcaraz PE, Rubio-Arias JA. Effects of resistance training movement pattern and velocity on isometric muscular rate of force development: a systematic review with meta-analysis and meta-regression. *Sports medicine*. 2020;50:943–963.
- 300 45. Rice DA, Mannion J, Lewis GN, McNair PJ, Fort L. Experimental knee pain impairs joint torque and rate of force development in isometric and isokinetic muscle activation. *European Journal of Applied Physiology*. 2019;119:2065–2073.
- 303 46. Turpeinen JT, Freitas TT, Rubio-Arias JÁ, Jordan MJ, Aagaard P. Contractile rate of force development after anterior cruciate ligament reconstruction—a comprehensive review and meta-analysis. *Scandinavian Journal of Medicine & Science in Sports*. 2020;30(9):1572–1585.
- 305 47. Helgerud J, Thomsen SN, Hoff J, Strandbråten A, Leivseth G, Unnhjem R, et al. Maximal strength training in patients with Parkinson's disease: impact on efferent neural drive, force-generating capacity, and functional performance. *Journal of Applied Physiology*. 2020;129(4):683–690.
- 307 48. Synek A, Lu SC, Vereecke EE, Nauwelaerts S, Kivell TL, Pahr DH. Musculoskeletal models of a human and bonobo finger: parameter identification and comparison to in vitro experiments. *PeerJ*. 2019;7:e7470.
- 309 49. Synek A, Pahr DH. The effect of the extensor mechanism on maximum isometric fingertip forces: A numerical study on the index finger. *Journal of Biomechanics*. 2016;49(14):3423–3429.
- 310 50. Qiu D, Kamper DG. Orthopaedic applications of a validated force-based biomechanical model of the index finger. In: 2014 36th Annual International Conference of the IEEE Engineering in Medicine and Biology Society. IEEE; 2014. p. 4013–4016.
- 312 51. Synek A, Lu SC, Nauwelaerts S, Pahr DH, Kivell TL. Metacarpophalangeal joint loads during bonobo locomotion: model predictions versus proxies. *Journal of the Royal Society Interface*. 2020;17(164):20200032.
- 314 52. Valero-Cuevas FJ, Cohn BA, Ingavson HF, Lawrence EL. Exploring the high-dimensional structure of muscle redundancy via subject-specific and generic musculoskeletal models. *Journal of biomechanics*. 2015;48(11):2887–2896. doi:10.1016/j.jbiomech.2015.04.026.
- 316 53. Song D, Raphael G, Lan N, Loeb GE. Computationally efficient models of neuromuscular recruitment and mechanics. *Journal of Neural Engineering*. 2008;5(2):008. doi:10.1088/1741-2560/5/2/008.
- 317 54. Tsianos GA, Rustin C, Loeb GE. Mammalian muscle model for predicting force and energetics during physiological behaviors. *IEEE Transactions on Neural Systems and Rehabilitation Engineering*. 2011;20(2):117–133.
- 319 55. Valero-Cuevas FJ, Towles JD, Hertz VR. Quantification of fingertip force reduction in the forefinger following simulated paralysis of extensor and intrinsic muscles. *Journal of biomechanics*. 2000;33(12):1601–1609.
- 321 56. Spoor C. Balancing a force on the fingertip of a two-dimensional finger model without intrinsic muscles. *Journal of Biomechanics*. 1983;16(7):497–504.
- 322 57. Sohrab HH. Basic Real Analysis. Birkhäuser Boston; 2003. Available from: https://books.google.com/books?id=gBPI_oYZoMMC.
- 323 58. Boyd S, Boyd SP, Vandenberghe L. Convex optimization. Cambridge university press; 2004.
- 324 59. Schneider CA, Rasband WS, Eliceiri KW. NIH Image to ImageJ: 25 years of image analysis. *Nature methods*. 2012;9(7):671–675.

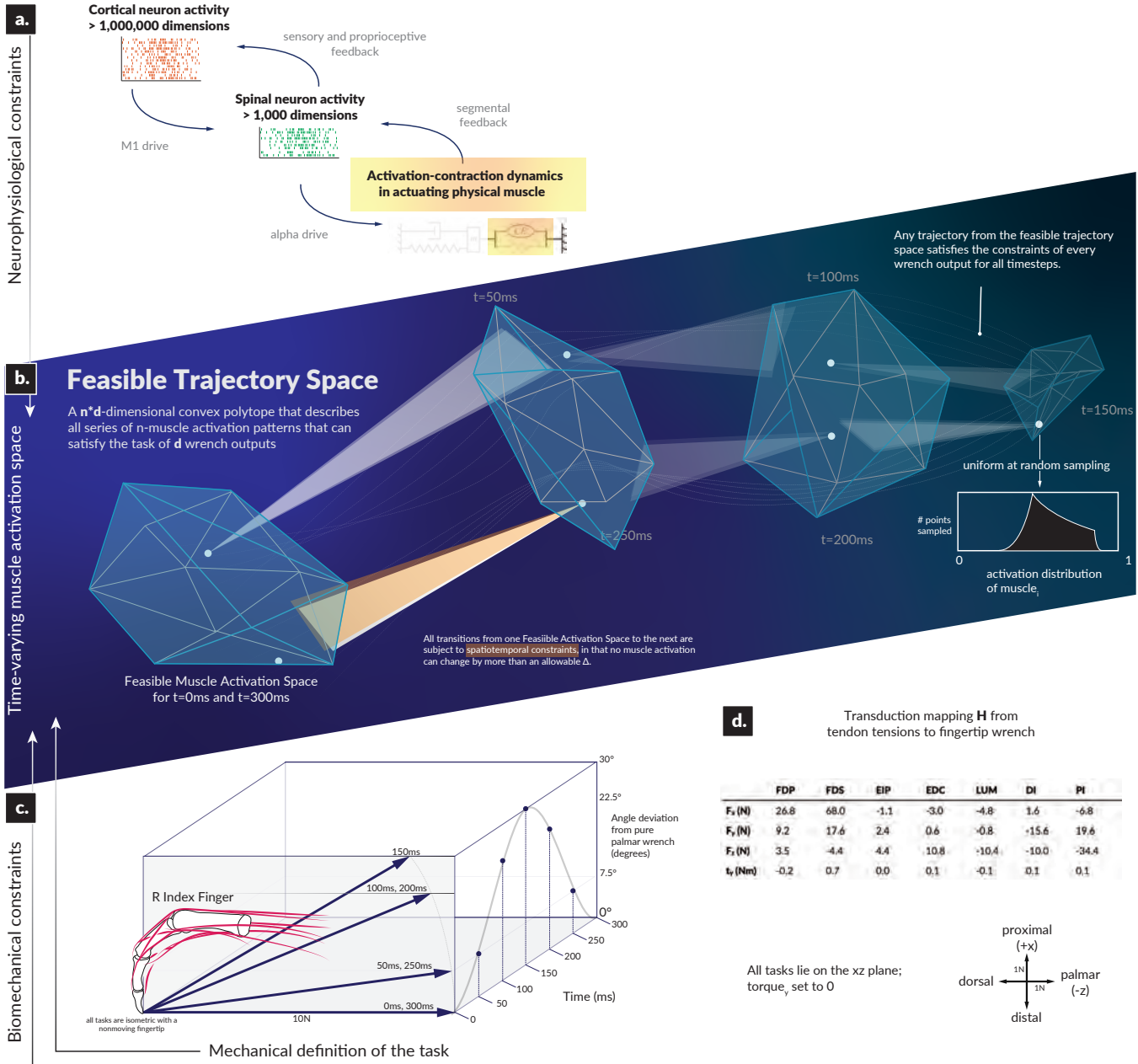


Fig. 1. The landscape within which motor learning and performance must occur in time is highly structured and spatially smaller than previously recognized. Our objective is to computationally survey the Feasible Trajectory Space in the context of activation-contraction constraint, to better inform our perspectives of descending neuromuscular control paradigms. We illustrate the types of neurophysiological constraints that affect muscle (a), highlight how a feasible activation space is subject to the aforementioned constraints (b), select a model system of a human cadaver index finger conducting a force redirection task (c) and document the model, as well as the axes (d). Illustrations in this summary figure are artistic representations.

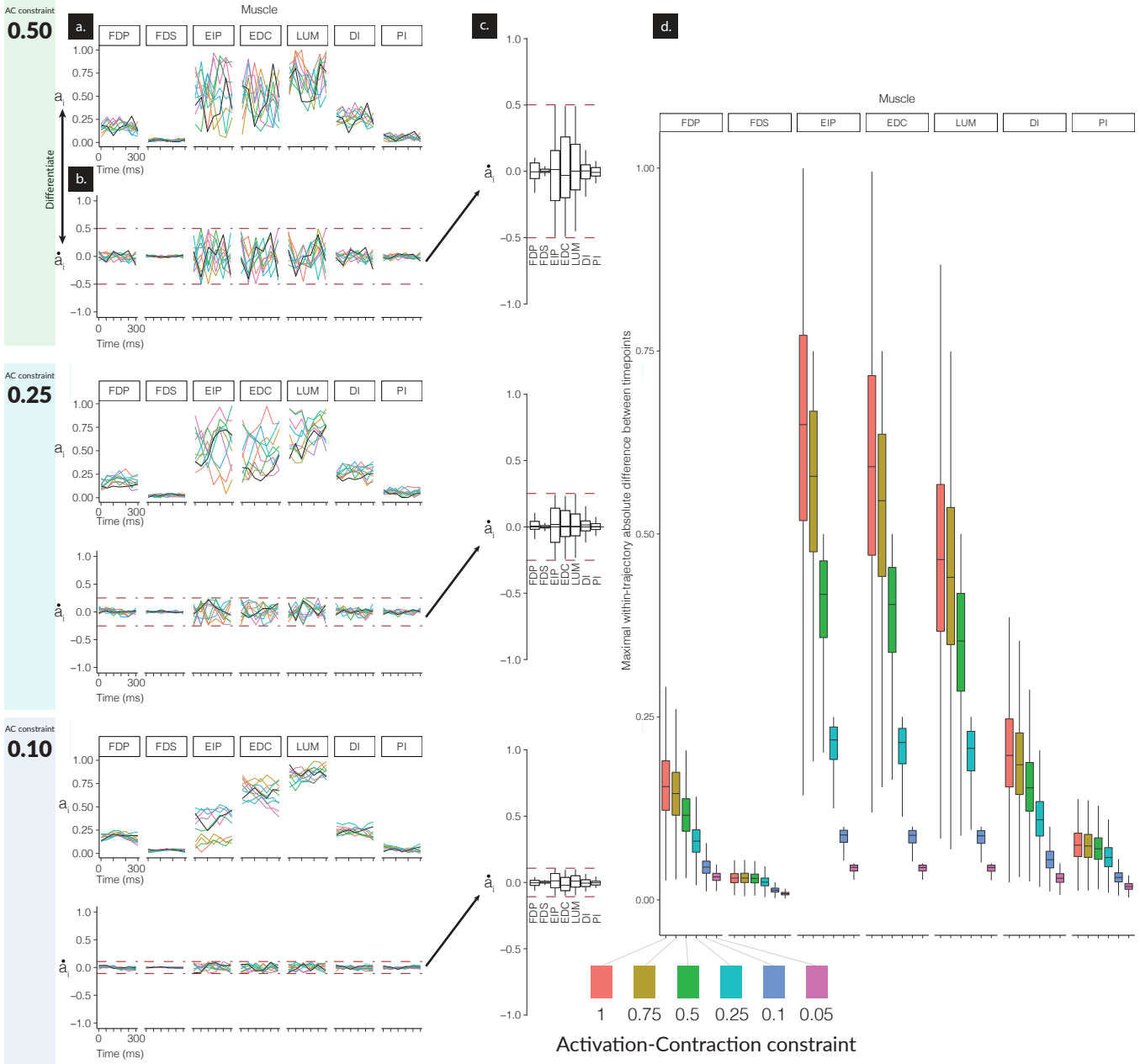


Fig. 2. Effect of tightening constraints on the feasible trajectory space. We show ten sample trajectories (from the 10,000 computed) for each of three levels of activation-contraction constraints For each activation-contraction level, we show a) sample trajectories, where each color is a different trajectory. b) Those trajectories, differentiated to show how quickly the activations were changing with the upper and lower activation-contraction constraints shown as dotted lines, and c) the full distribution ($n=10,000$) of the trajectory 'activation-contraction speeds', grouped by muscle. Note that colors on part c) do not relate to a) and b). Outliers are not shown on c). In d), we show the effect of differing activation-contraction constraints on the distribution of $\max(|\dot{a}_i|)$, compared across muscles. When we sample trajectories, we get n -dimensional trajectories, with $n=7$ muscles. From each of those trajectories, we differentiate them (e.g. $\dot{a}_i = a_{i+1}^{LUM} - a_i^{LUM}$), and we show here the distributions of e.g. \dot{a}^{LUM} . These speeds are grouped by the applied activation-contraction constraint. The case with no activation-contraction constraints is a 1.0; a 0.1 means a muscle is spatiotemporally constrained so that it cannot change by more than 10% within 50ms.

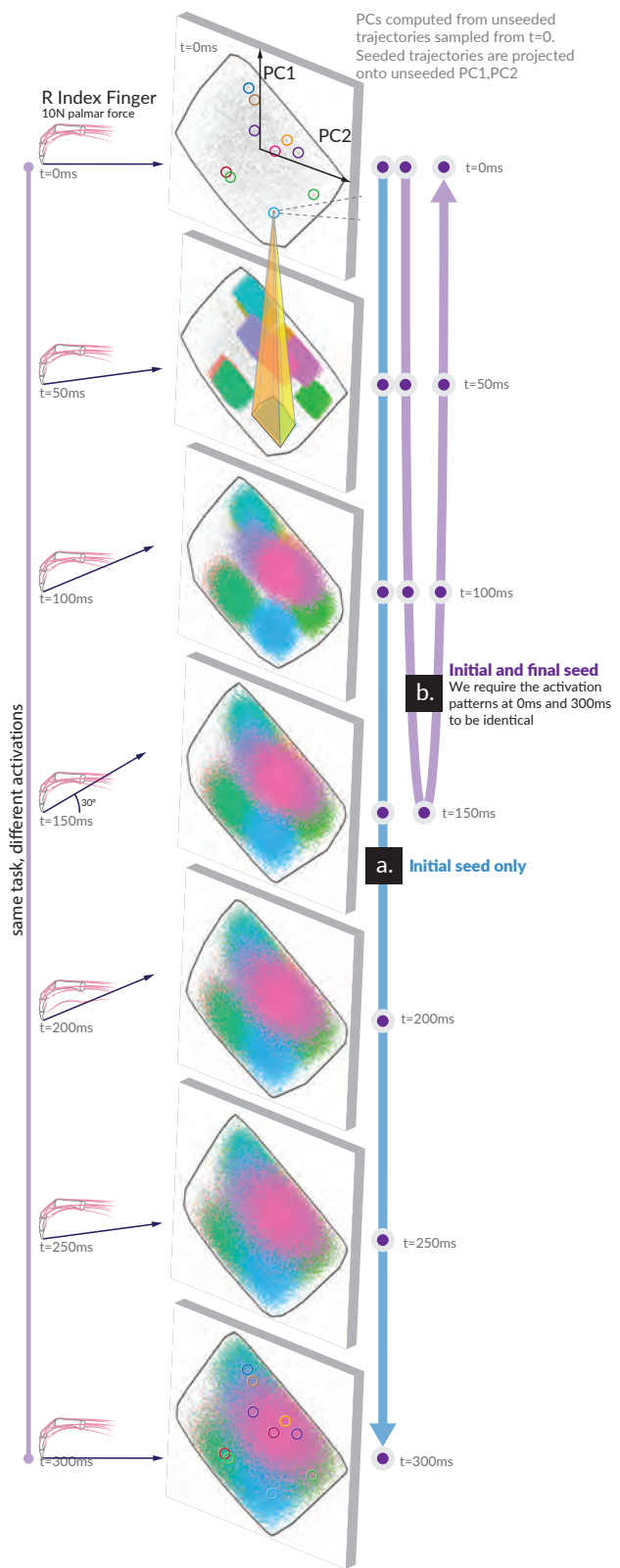


Fig. 3. hi